

Hybrid Side-branch Resonator based Acoustic Metamaterials for Broad and Flat Bandgap in Sound Transmission

Lee, Soo Yeong¹

School of Mechanical Engineering, Chungnam National University
99 Daehak-ro, Yuseong-gu, Daejeon 34134, South Korea

Lee, Joong Seok²

School of Mechanical Engineering, Chungnam National University
99 Daehak-ro, Yuseong-gu, Daejeon 34134, South Korea

ABSTRACT

Sound transmission through long and narrow ducts is one of the typical but important issues in acoustic treatments. Recently, acoustic metamaterials has attracted much attention in noise reduction owing to providing unusual tailoring of sound wave. For examples, arrays of subwavelength resonators along a duct reduce sound transmission substantially by forming bandgaps in which effective bulk modulus becomes negative values. For a broader and flatter bandgap, however, more number of dissimilar resonators should be installed in a dedicate manner, such that a larger space is inevitably required along the duct. To cope with the difficulty, we propose a novel acoustic metamaterial based on hybrid side-branch resonators in order to exhibit a broad and flat bandgap in sound transmission in a compact scale. Each hybrid resonator in the proposed acoustic metamaterial consists of parallel subbranches with varying lengths. Because combined resonances between adjacent side branches as well as local resonances in individual ones affect the bandgap formation, specific arrangements of hybrid resonators are also studied to broaden and flatten the target bandgap. The effective medium theory is applied to model the proposed acoustic metamaterial and numerical studies are carried out to investigate the effects of geometric parameters.

Keywords: Acoustic metamaterial, Sound transmission reduction, Bandgap, Side-branch resonator

I-INCE Classification of Subject Number: 37

1. INTRODUCTION

Since sound propagation through long and narrow ducts may cause serious noise problem in many applications, there have been various treatments for efficient reduction of sound transmission [1]. Contrary to conventional treatments [1], new approaches based on exotic wave propagation phenomena using metamaterials have been demonstrated both numerically and experimentally in the last decades [2,3]. For examples, extraordinary acoustic parameters such as negative mass density and negative bulk

¹ sooylee@cnu.ac.kr

² jsleecnu@cnu.ac.kr

modulus that cannot exist in natural materials were realized by using membranes [4-6], Helmholtz resonators [7,8] or side-branch resonators [9-12]. Among them, we are here interested in a periodic arraying of side-branch resonators, which form sound transmission bandgap where the effective bulk modulus becomes negative values.

Figures 1(a) and 1(b) show identical ducts installing side branches with difference lengths (h_1, h_N), while Fig. 1(c) shows the same duct with an array of length-varying side branches. Since the bandwidth of sound transmission bandgaps are decided by the length of the installed side branches, the length-varying side branches produces a broader bandgap, resulting in the enhancement of transmission loss (TL), as shown in Figs. 1(d) and 1(e), respectively. Thereby, we employ the length-varying side branches shown in Fig. 1(c) as a basis for the proposed metamaterials.

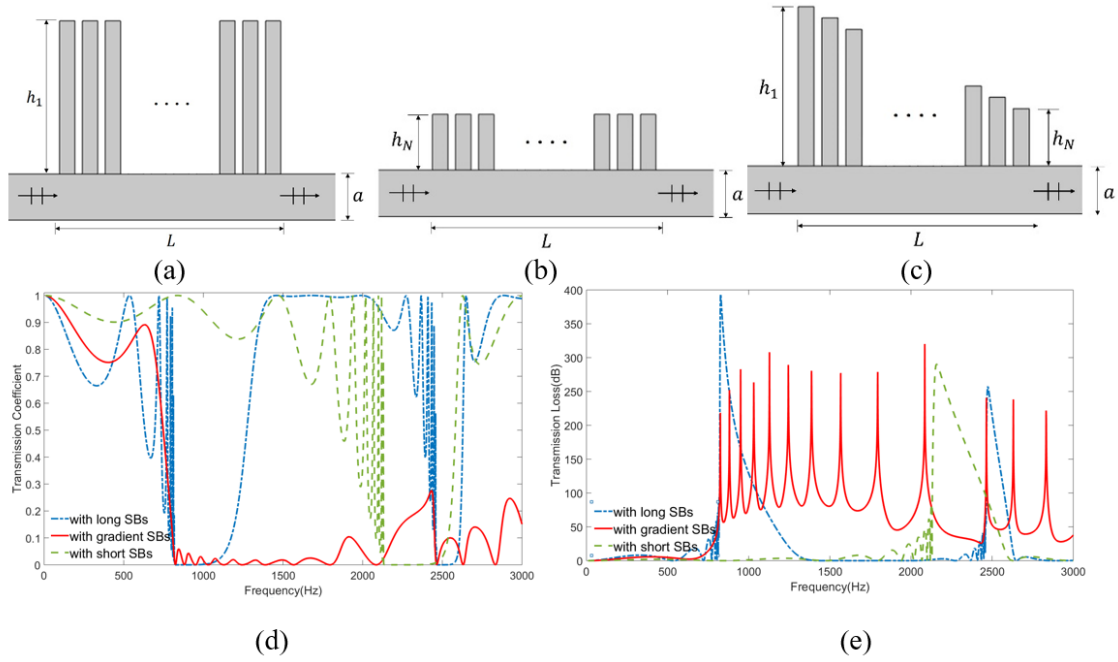


Figure 1. (a) A narrow duct (diameter a) with long side branches (length h), (b) a duct with short side branches, (c) a duct with length-varying side branches, (d,e) a comparison of (d) sound transmission coefficients and (e) sound transmission loss (TL) of the ducts with different types of side branches.

2. AN EFFECTIVE MEDIUM MODEL

Since the basis of the metamaterials is composed of periodic side-branch resonators in this work, we can model the metamaterial as effective layers by using the effective medium theory [9,13-15] as shown in Fig. 2(a).

To build the effective model for the duct with periodic arrays of length-varying side branches, the region containing a side-branch resonator can be modelled as an effective medium illustrated as a region B in Fig. 2(a). Note that the region B contains the side branch filled with air (ρ_0) and the rigid part outside of the side branch (ρ_{rigid}). Then, the effective density ρ^s of the region B can be expressed as

$$\frac{1}{\rho^s} = \frac{\eta}{\rho_0} + \frac{(1-\eta)}{\rho_{rigid}}, \quad (1)$$

where η denotes the volume ratio of the side branch (air) part compared to the region B ($0 < \eta \leq 1$). Since $\rho_{rigid} = \infty$, the effective density of the region B can be found to be

$$\rho^s = \frac{\rho_0}{\eta}. \quad (2)$$

In the similar manner, the effective bulk modulus K^s of the region B can be expressed as

$$\frac{1}{K^s} = \frac{\eta}{K_0} + \frac{(1-\eta)}{K_{rigid}}, \quad (3)$$

$$K^s = \frac{K_0}{\eta}. \quad (4)$$

Then, the effective sound velocity c^s in the region B can be obtained as

$$c^s = \sqrt{K^s / \rho^s} = c_0.$$

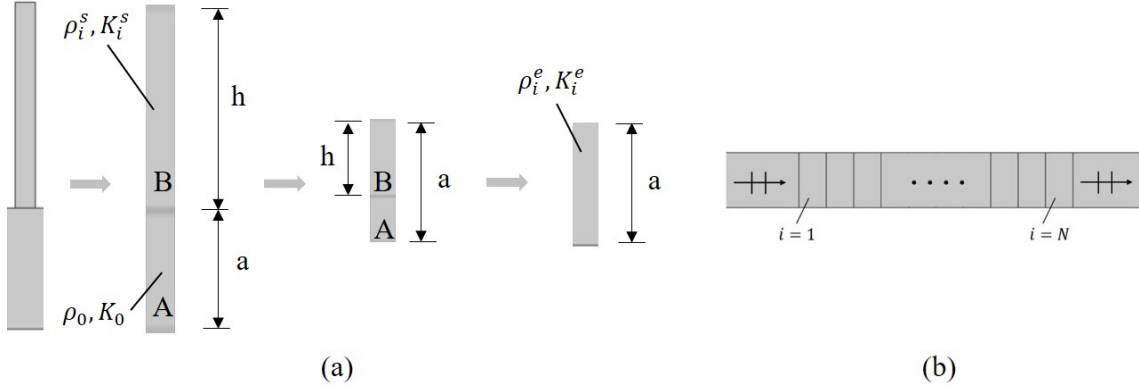


Figure 2. (a) The unit cell configuration modelled as effective medium. (b) Proposed metamaterial represented as effective layers of different material properties.

Owing to the various length of side branches in unit cell, we model each effective layer (denoted by the subscript i) with different material properties as illustrated in Fig. 2(b). The effective material properties of each layer can be obtained by considering wave interaction between the regions A and B. The region B can be regarded as a pipe closed on one end whose surface acoustic impedance [16] at interface ($y = a$) from the side hard wall ($y = h$, $i = 1, 2, \dots, N$) is given by

$$Z_{Bi} = -j\rho^s c^s \cot(kh_i) = -j \frac{\rho_0 c_0}{\eta} \cot(kh_i), \quad (5)$$

where k is the wavenumber of air.

In the region A, sound wave propagates along the x direction and oscillates along the y direction, therefore the pressure field and particle velocity in the region A of the i th layer can be written as

$$p_{Ai} = C_i \cos(k_{iy} y) e^{-jk_{ix} x}, \quad (6)$$

$$v_{Aiy} = \frac{C_i}{j\omega c_0} \sin(k_{iy} y) e^{-jk_{ix} x} = \frac{C_i k_{iy}}{j\omega \rho_0} \sin(k_{iy} y) e^{-jk_{ix} x} \quad (7)$$

At the interface between the regions A and B ($y = a$), the pressure and velocity fields should meet condition of continuity, which is derived as

$$\left(\frac{p_{Ai}}{v_{Aiy}} \right)_{y=a} = Z_{Bi}, \quad (8)$$

$$\frac{\cos(k_{iy}a)}{\frac{k_{iy}}{j\omega\rho_0}\sin(k_{iy}a)} = -j\frac{\rho_0c_0}{\eta}\cot(kh_i), \quad (9)$$

$$-k_{iy}\tan(k_{iy}a) = \eta k \tan(kh_i). \quad (10)$$

In a low frequency range, equation (10) can be expressed in the wave vector components, which satisfy $k_i^2 = k_{ix}^2 + k_{iy}^2$ as

$$k_{iy}^2 = -\frac{\eta k \tan(kh_i)}{a}, \quad (11)$$

$$k_{ix} = k\sqrt{1 + \eta \tan(kh_i)/ka}. \quad (12)$$

Then, the effective acoustic density, the effective sound velocity, and the effective bulk modulus of the proposed metamaterial can be obtained as

$$\frac{1}{\rho_i^e} = \frac{(1-\phi)}{\rho_0} + \frac{\phi}{\rho^s} \quad (13)$$

$$c_i^e = \frac{\omega}{k_{ix}} = \frac{c_0}{\sqrt{1 + \eta \tan(kh_i)/ka}} \quad (14)$$

$$K_i^e = \rho_i^e (c_i^e)^2 = \frac{c_0^2}{\left(\frac{(1-\phi)}{\rho_0} + \frac{\phi}{\rho^s}\right) \left(1 + \frac{\eta \tan(kh_i)}{ka}\right)}. \quad (15)$$

where ϕ is the ratio of the side-branch length to the whole metamaterial height $[h_i/(a+h_i)]$.

Fig 3(a) and 3(b) show the effective bulk moduli K^e in the effective layers calculated from equation (15). As shown in Fig. 3(a), we observe that the effective bulk moduli K^e become negative at a certain frequency 822Hz for the long side-branch model and 2,137Hz for the short side-branch model, the frequencies correspond to the starting frequencies of their bandgaps. In the length-varying side-branch model, effective bulk moduli K^e become negative at different frequencies forming broad bandgap because each layer has different effective material properties as shown in Fig. 3(b).

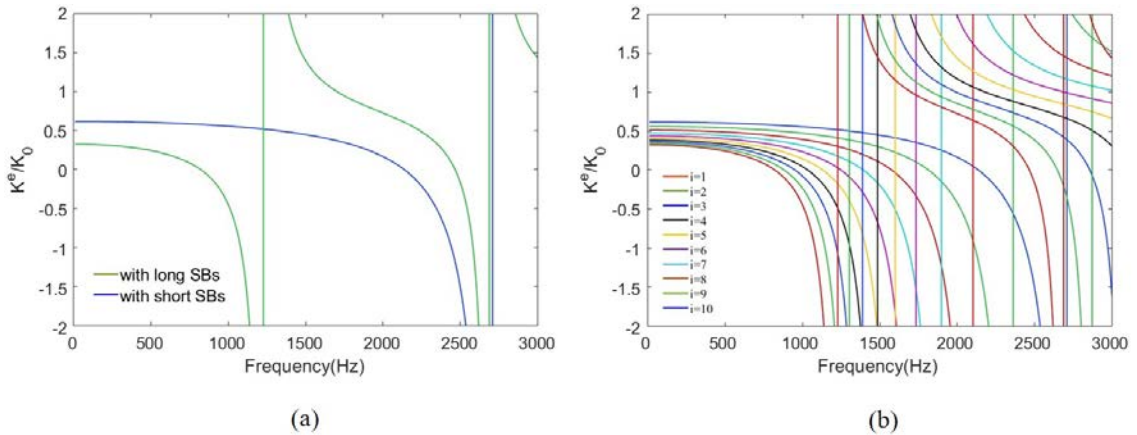


Figure 3. (a) Effective bulk modulus (normalized by that of air) of the duct with long side branches (blue) and that with short side branches (green). (b) Effective bulk modulus of each layer of the metamaterial duct with length-varying side branches ($i = 1, 2, \dots, N$).

3. DESIGNS AND RESULTS

Various parametric studies are carried out to investigate relations between the sound transmission reduction performance and geometric parameters.

- ✓ A larger gradient in side-branch lengths makes a broader bandgap but provokes more fluctuations
- ✓ More number of side branches make a flatter bandgap
- ✓ Thinner side branches make more fluctuating bandgap

For a broader and flatter bandgap, more number of dissimilar resonators is required, but more number of resonators generally need a larger space along the duct. To deal with the difficulty, we propose a novel acoustic metamaterial based on hybrid side-branch resonators in order to present a broad and flat bandgap in sound transmission. As illustrated in Fig. 4(a) or 4(b) the hybrid resonators are constructed by splitting each side branch down to the duct, such that each hybrid resonator consists of paralleled subbranches with varying length.

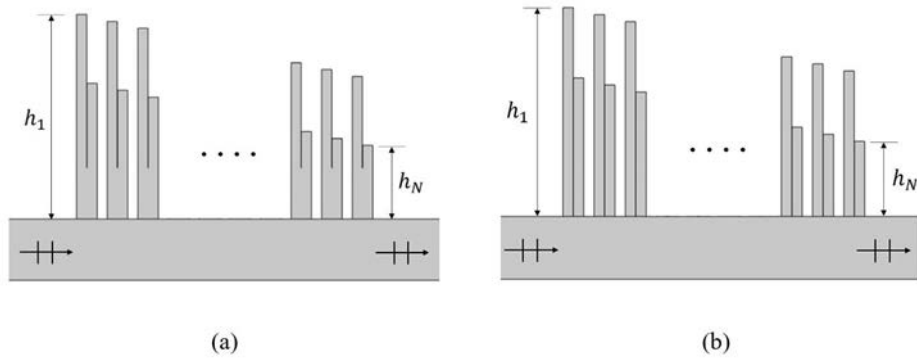


Figure 4. Illustration of hybrid side-branch resonators.

As shown in Fig. 5(a), the sound transmission bandgap of the proposed metamaterial with hybrid side-branch resonators is flatter than other duct models. In Fig. 5(b), the sound transmission loss (TL) for the present metamaterial with the hybrid side-branch resonators also increases compared to those of other models. With the hybrid side-branch resonators, however, unusual peaks and dips appear owing to Fabry–Pérot resonance between adjacent side branches.

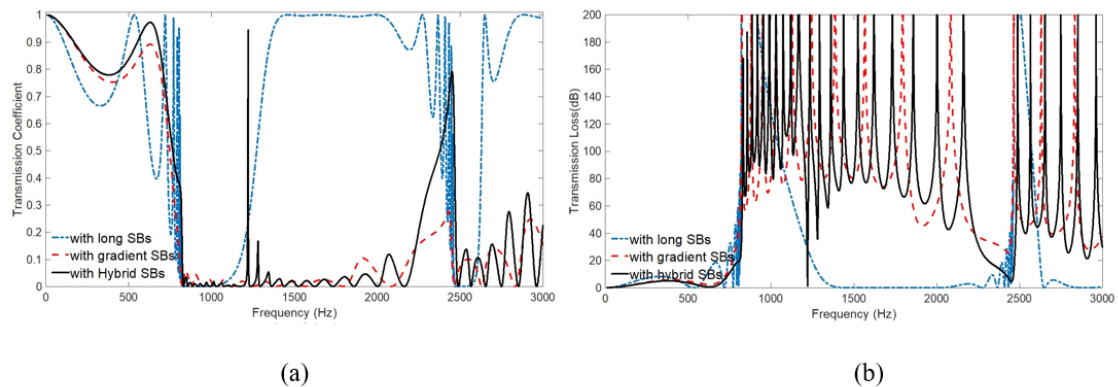


Figure 5. Comparison of (a) sound transmission coefficient and (b) sound transmission loss (TL) of the proposed metamaterial duct compared to nominal ones.

4. CONCLUSIONS

In this study, we intend to make a broader and flatter sound transmission bandgap by arraying side-branch resonators along the duct. To enhance the sound transmission reduction performance, we propose the hybrid resonator that indicates broader and flatter bandgap than previous designs except unusual Fabry–Pérot resonances between adjacent side branches.

5. ACKNOWLEDGEMENTS

This research was supported by Basic Science Research Program through the National Research Foundation of Korea (NRF) funded by the Ministry of Education (Grant No.: 2018R1D1A1B07049771).

6. REFERENCES

1. I. L. Vér and L. L. Beranek, “*Noise and Vibration Control Engineering: Principles and Applications*”, John Wiley & Sons, Inc. (2006).
2. Z. Liu, X. Zhang, Y. Mao, Y. Y. Zhu, Y. Zhiyu, C. T. Chan and P. Sheng, *Science* **289**, 1734-1736 (2000)
3. N. Fang, D. Xi, J. Xu, M. Ambati, W. Srituravanich, C. Sun and X. Zhang, *Nat. Mater.* **5**, 452-456 (2006)
4. Z. Yang, J. Mei, M. Yang, N. H. Chan and P. Sheng, *Phys. Rev. Lett.* **101**, 204301 (2008)
5. F. Ma, J. H. Wu, M. Huang, W. Zhang and S. Zhang, *J. Phys. D: Appl. Phys.* **48**, 175105 (2015)
6. G. Ma, M. Yang, S. Xiao, Z. Yang and P. Sheng, *Nat. Mater.* **13**, 873-878 (2014)
7. Y. Cheng, J. Y. Xu and X. J. Liu, *Phys. Rev. B* **77**, 045134 (2008)
8. C. M. Park and S. H. Lee, *Appl. Phys. Lett.* **102**, 241906 (2013)
9. J. Yang, J. S. Lee and Y. Y. Kim, *J. Phys. D: Appl. Phys.* **50**, 015301 (2017)
10. V. M. García-Chocano, R. García -Salgado, D. Torrent, F. Cervera and J. Sánchez-Dehesa, *Phys. Rev. B* **85**, 184102 (2012)
11. X. J. Li, C. Xue, L. Fan, S. Y. Zhang, Z. Chen, J. Ding and H. Zhang, *Appl. Phys. Lett.* **108**, 231904 (2016)
12. S. K. Tang, *J. Acoust. Soc. Am.* **132**, 3086 (2012)
13. J.-P. Groby, W. Huang, A. Lardeau and Y. Auréggan, *J. Appl. Phys.* **117**, 124903 (2015)
14. J. Yang, J. S. Lee and Y. Y. Kim, *J. Appl. Phys.* **117**, 174903 (2015)
15. J. Yang, J. S. Lee, H. R. Lee, Y. J. Kang and Y. Y. Kim, *Appl. Phys. Lett.* **112**, 091901 (2018)
16. Trevor J. Cox and P. D’Antonio, “*Acoustic Absorbers and Diffusers: Theory, Design and Application*”, CRC Press (2004)